Yabra Melina Sol (Orcid ID: 0000-0003-1614-778X)

Observational study of the South American Low-Level Jet during the SALLJEX

Yabra, Melina Sol[A B C *], Matilde Nicolini[A D E], Paloma Borque[F], Yanina Garcia Skabar[B C E], Paola Salio[A D E]

[A] Universidad de Buenos Aires, Facultad de Ciencias Exactas y Naturales, Departamento de Ciencias de la Atmósfera y los Océanos (UBA-FCEN-DCAO), C1428EGA, Buenos Aires, Argentina.

[B] Servicio Meteorológico Nacional, C1425GBE, Buenos Aires, Argentina.

[C] Consejo Nacional de Investigaciones Científicas y Técnicas (CONICET), C1033AAJ, Buenos Aires, Argentina.

[D] Centro de Investigaciones del Mar y la Atmósfera (CIMA), CONICET – UBA, C1428EGA, Buenos Aires, Argentina.

[E] Instituto Franco Argentino Sobre Estudios de Clima y Sus Impactos (UMI-IFAECI/CNRS-CONICET-UBA), C1428EGA, Buenos Aires, Argentina.

[F] Pacific Northwest National Laboratory, Richland, WA, USA.

* Corresponding author. Melina Sol Yabra, Servicio Meteorológico Nacional, Av. Dorrego 4019, Buenos Aires City, República Argentina, C1425GBE. myabra@smn.gob.ar

Keywords: Low-Level Jet, SALLJ, South America, SALLJEX

Abstract

The South American Low-Level Jet (SALLJ) is a narrow northerly wind speed maximum present just above the boundary layer. It is an important component of the tropical-extratropical heat and moisture exchange in South America and can favor deep moist convection in Southeastern South America. The main objective of this study is to analyze the SALLJ characteristics at 21 upper-air stations deployed between the tropics and the subtropics from just east of the Andes to the eastern plains during the SALLJ Experiment (SALLJEX). The greatest wind speed occurs between 300 m and 2000m AGL between 03 and 12 UTC, mainly in connection with greater northerly winds during an anticlockwise rotation of the wind from sunset to sunrise, thus suggesting the important role of the inertial oscillation in the wind's diurnal cycle. The spatial variation of the LLJ throughout the SALLJEX network shows a weakening of the maximum wind speed from stations near the Andes towards the Plains suggesting the presence of the LLJ core just east of the Andes around Santa Cruz de la Sierra's latitude (17°48'S). Weak, moderate, and strong SALLJ categories defined from a local maximum northerly wind speed threshold at each station are defined to analyze the relationship between the SALLJ intensity and the thermodynamic properties of the lower layers of the atmosphere. Strong SALLJs are frequently observed at nighttime, while weak SALLJs are likely to occur at any time of the day. Strong cases have deeper and less stable nocturnal boundary layers, which could be due to the SALLJ warm advection near the time of wind speed maximum (06 UTC). Deeper convective boundary layers and higher low-level temperatures observed at 18 UTC prior to strong nocturnal SALLJs can potentially lead to larger amplitudes of inertial oscillation and contribute to generating stronger SALLJs.

1. Introduction

The low-level jet (LLJ) is a wind speed maximum that occurs in the lowest few kilometers of the atmosphere and is associated with vertical and horizontal shear (Stensrud, 1996). The LLJ is a key component of the Earth's climate as it can favor the development of deep moist convection by transporting warm and moist air and promoting ascent in the jet exit region (e.g., Means, 1954; Stensrud, 1996; Gimeno et al., 2016; Algarra et al., 2019; Braz et al., 2021). LLJs are also important due to their effect on aerosols dispersion (Wei et al., 2018, Ulke et al., 2014), birds' migration (Wainwright et al., 2016), aviation safety (Arkel, 2000; Madougou et al., 2014), and wind energy (Gutierrez et al., 2014; Gadde and Stevens, 2021). Stensrud (1996), Paegle (1998), Shapiro et al. (2016) and Braz et al. (2021) reviewed and synthesized more than six decades of LLJ studies worldwide. According to these studies, the nocturnal inertial oscillation resulting from the decoupling of the residual layer from the stable boundary layer (Blackadar 1957) is an important mechanism in the LLJ formation over the U.S. Great Plains. In agreement with Blackadar (1957), the maximum wind speed takes place at night or around dawn hours before convective turbulence reaches the LLJ height. Other studies have shown different LLJ generation or controlling mechanisms that can complement or oppose the inertial oscillation (e.g., Parish and Oolman, 2010; Van de Wiel et al., 2010; Klein et al., 2015). Efforts continue to improve the characterization of the LLJ to validate and/or improve its representation in numerical weather forecast models. To this day, these numerical models fail to correctly reproduce the LLJ, by underestimating its intensity or overestimating its height (e.g., Shapiro et al., 2016).

The South American low-level let (SALLJ) east of the Andes (Vera et al., 2006) plays a crucial role in the hydrological cycle over Southeastern South America (SESA) due to its impact on precipitation (e.g. Douglas et al., 1998; Salio et al., 2002; Marengo et al., 2004; Nascimento et al., 2016; Gimeno et al., 2017). The SALLJ is an important component of the tropical-extratropical exchange of

heat and moisture in South America that favors the occurrence of deep moist convection in SESA. Convection is favored by low-tropospheric air ascent in its exit region or when it intercepts mountain ranges. It can also promote deep moist convection over regions where humid and thermodynamic unstable air masses are advected by the SALLJ (Velasco and Fritsch, 1987; Salio et al., 2007; Rasmussen and Houze, 2011, 2016; Repinaldo et al., 2015, 2017).

Observational evidence for the SALLJ is scarcer than in North America. This is in part due to the sparser coverage and fewer operational upper-air observations over South America (Paegle, 1998). Despite this limitation, the SALLJ was first observed and documented during the early 1980s (Litchenstein, 1980; Virji, 1981; Fernandez and Necco, 1982). Inzunza and Berri (1991) studied 1973-1974 wind profiles over northern Argentina with pibals and radiosondes launched at 00 UTC (21 LT - near sunset) and 12 UTC (09 LT - near sunrise) from Salta and Resistencia operational weather stations (Fig. 1). In that study, they found that a stronger SALLJ was observed over Northeast Argentina at sunrise (in agreement with what is expected from inertial oscillation), and a weaker one closer to the Andes at sunset. Douglas et al. (1998) analyzed wind profiles from January to March 1998 at Santa Cruz de la Sierra (Fig. 1) with maximum intensity between 1 and 2 km above ground level (AGL), stronger, higher, and deeper in the late afternoon (21 UTC – 17 LT) than in the early morning (11-13 UTC – 7-9 LT). However, the reduced number of morning soundings they analyzed could have hampered the ability to characterize the SALLJ diurnal cycle by biasing the results towards an afternoon wind maximum. In fact, Marengo et al. (2002) used upper-air observations from the next summer (1999) at the same station and found stronger wind speed maxima at 11-13 UTC and weaker winds at 20-22 UTC. Oliveira et al. (2018) identified SALLJ profiles in a 20-year dataset of radiosondes at 00 and 12 UTC locately mostly over eastern Brazil and Argentina. This climatological study revealed the presence of elevated

SALLJs between 1500 m and 3000 m AGL from the north and west directions likely related to synoptic-scale baroclinic systems (Campetella and Vera, 2002). Recently, Sasaki et al. (2022) identified SALLJ events from two sounding sites in central-north Argentina from the Remote sensing of Electrification, Lightning, And Mesoscale/microscale Processes with Adaptive Ground Observations - Clouds, Aerosols, and Complex Terrain Interactions field campaigns (RELAMPAGO-CACTI, Nesbitt et al. 2021; Varble et al. 2021). In agreement with previous studies, they showed that SALLJs most frequently come from the north, occur overnight, and reach their maximum wind speed below 850 hPa for boundary layer LLJs and between 850 hPa and 550 hPa for elevated LLJs. This shows that despite previous observational work aiming to characterize the SALLJ, its diurnal wind cycle, time of wind maximization, maximum wind speed, and associated height above the ground vary depending on the region. To this day, no previous studies have explored these aspects from observations at several stations over a region east of the Andes extending from 7°S to 35°S. The sparsity of the operational upper-air observation network over SESA leads to errors in representing the SALLJ vertical structure, its core position, and intensity which results in uncertainties in humidity and heat fluxes that have a significant impact on weather prediction in the region (Wang and Paegle, 1996; Marengo et al, 2004; Rife et al, 2010). Because of these disadvantages in the observational coverage and frequency of upper-air observations in the region, many descriptions of the SALLJ are based on operational analyses or reanalyses (Elthair and Bras, 1994; Wang and Paegle, 1996; Nogues-Paegle and Mo, 1997; Douglas et al., 1998). However, a dense upper-air observational network is still required for rigorous validation of numerical models. This motivated the SALLJ Experiment (SALLJEX, Vera et al., 2006) that led to a considerable increase of the spatial and temporal density of pibals and radiosonde measurements over SESA during the 2002-2003 austral warm season. SALLJEX resulted in the addition of 22 upper

air measuring stations and more frequent radiosonde launches in all operational stations. This enhanced upper-air network formed by 25 stations covered a region from the tropics (Cruzeiro do Sul, 7.63ºS, 72.7ºW) to the subtropics (Paraná, 31.83ºS, 31.83ºW) and from just west of the Andes (Piura, 5.2ºS 80.6ºW) to the eastern plains (Foz do Iguaçu, 24.5ºS 54.6ºW) (Fig. 1). SALLJEX represents the densest upper-air network in this region to this day and it is crucial in the documentation of the structure of the SALLJ in a region large enough to cover its variations due to synoptic variability.

This study presents a comprehensive observational analysis of the SALLJ from SALLJEX upper-air observational network. Given the highest temporal and spatial density of upper-air observations during the SALLJEX's upper-air network, the objectives of this work are two-folded. First, to provide an observational description of the spatial configuration of the LLJ timing, peak speed, direction, and height over SESA during the SALLJEX. Here, emphasis is placed on describing two-way effects between the LLJ and the spatial variability of the low-level thermodynamics as well as their diurnal cycle. Second, to explore the relationship between the nighttime SALLJs strength and the low-level vertical thermodynamic structure. The analyses provided in this work can facilitate the validation of different boundary-layer parameterizations leading to a better representation of the SALLJ in numerical weather models.

This paper is organized as follows: the dataset is presented in Section 2. The methodology is described in Section 3. The analysis of the mean SALLJEX profiles is shown and discussed in Section 4 and the analysis of different SALLJ categories is shown in Section 5. Lastly, the summary and conclusions of this work are provided in Section 6.

2. Data

The SALLJEX was an international field campaign aimed to describe many aspects of the SALLJ (Vera et al., 2006). This field campaign took place over Bolivia, Paraguay, Peru, central and northern Argentina, and western Brazil during the 2002-2003 austral warm season. Between November 15, 2002, and February 15, 2003, SALLJEX deployed a regional network of radiosonde, pibal, and pluviometer sites, as well as flights from NOAA WP3 over Bolivia and Argentina. Most upper-air observations from radiosondes and pibals stations were located along the SALLJ core (Fig. 1). Ica, Piura, and Puno stations were not included in this work because their location over the slope, or to the west, of the Andes mountain range is not influenced by the SALLJ. The same reason applies to Salta station which was also not included in this analysis due to its location in the Lerma valley at 1152 m above mean sea level (AMSL). During the entire observational period, radiosondes were launched daily at 06 UTC and pibals twice a day at 12 and 21 UTC. From January 6 to February 15, 2003, a Special Observation Period (SOP) took place during which pibals and radiosondes were launched according to the timing described in Table 1. In addition, during Intensive Observation Periods (IOPs) the observation frequency increased to three or four radiosondes and eight pibals per day at selected locations (Table 1). IOPs occurred when an intense SALLJ event was expected, thus the wind speed measurements during these periods are likely to be skewed towards higher values. During IOP days a total of 8 observations were scheduled at stations with pibals and radiosondes with only one measurement per time. Non-operational stations in Brazil (Dourados, Rio Branco, Vilhena, Cruzeiro do Sul) started to measure on January 1, 2003, thus reducing the number of available observations at these stations. Lastly, Foz do Iguaçu only had twice daily operational radiosonde observations. SALLJEX data was thoroughly quality controlled (García Skabar and Nicolini, 2009).

All radiosonde and pibal measurements were linearly interpolated every 100 m to the same height above mean sea level (AMSL). Thus, analyses shown herein refer to heights AMSL unless explicitly stated. Radiosonde provided wind, temperature, humidity, and pressure vertical profiles while pibals only provided wind vertical profiles. Figure 2 shows the number of observations at each station as a function of time measured by radiosondes (Fig 2a, thermodynamic variables) and by radiosondes and pibals (Fig. 2b, wind variables). The higher number of upper-air observations was registered in Mariscal Estigarribia, Chamical, Resistencia, and Santiago del Estero stations, which was in part due to these stations launching more radiosondes at 06 UTC than any other station (Fig. 2). A noticeable decrease in the number of observations from pibals was registered in all stations at nighttime (between 00 and 09 UTC). It is necessary to clarify that not all measurements reach the same maximum height. Observations from radiosondes could reach heights higher than 10 km, while observations from pibals could end at any height due to tracking difficulties. Several factors can affect pibals, amongst them are a low cloud base height and rain occurring at the time of the measurement. Nocturnal pibals present an additional challenge due to the measurement method. At nighttime, the balloon carries a small light that the observer has to manually track with a theodolite. Following this light on a bright starry night is a difficult task that often results in scant observations. Pibal-retrieved vertical profiles of zonal and meridional wind components are derived from repeated annotations (every 30 seconds during the first 8 minutes and then every 1 minute) of the elevation and the azimuth angle while the balloon freely ascends by buoyancy. The height was calculated assuming a constant ascent rate of 3.2 m s^{-1} for the 30 g balloons used during SALLJEX (Galvez et al., 2005). Variations in the ascent rate of the balloons can lead to small uncertainties (~10%) in the wind profiles (Douglas et al., 1998).

3. Methodology

This work includes two different wind profile analyses at each station. The first one analyzes all wind profiles collected during the SALLJEX period and focuses on the local maximum without specifying its direction (called 'LLJ' from now on). The second analysis concentrates only on wind profiles that present a local maximum with a northerly component (a negative meridional component of wind - 'SALLJ' from now on). The SALLJs are categorized according to their maximum wind speed. Then, the SALLJ intensity, structure, and variability during the field campaign are analyzed. Bonner (1968) proposed a criterion to define a LLJ based on different thresholds for its maximum wind speed in the lowest 1500 m AGL and wind shear thresholds above that maximum. In South America, previous studies have identified SALLJ events by applying the Bonner criteria to reanalysis data (e.g., Sugahara et al., 1994; Marengo et al., 2002; Marengo et al., 2004; Nascimento et al., 2016). Oliveira et al. (2018) and Sasaki et al. (2022) modified these criteria to be more flexible by deepening the layer for LLJ identification to 3000 m and 3200 m AGL respectively. These criteria allowed more days with SALLJs to be identified throughout South America including more instances of elevated SALLJs. Although several thresholds of wind speed and shear have been used in those studies, Montini et al. (2019) argued that these fixed thresholds can introduce biases in the identification of SALLJ events given its significant seasonal and spatial variability. Therefore, Montini et al. (2019) generated a new SALLJ climatology based on the 75th percentiles of wind speed and wind shear at two SALLJEX stations (Santa Cruz de la Sierra and Mariscal Estigarribia) still using fixed pressure levels similar to the conventional Bonner criteria.

This work builds on Montini et al. (2019) by analyzing observations from all the SALLJEX stations located along the SALLJ core at all available times. Thus, a better temporal and spatial representation of the SALLJ purely from

observations is possible herein. As mentioned in Section 1, a new kinematic classification is defined in this work. To determine which observations correspond to SALLJ profiles, the following selection criteria are used:

1. Each measured wind profile is smoothed using a 5-point moving average to remove the noise associated with the pibal or small-scale turbulence (Arya, 2005; He et al., 2020).
2. Wind speed local maxima up to 3000 m AMSL are identified in the smoothed profile.
3. The strongest identified wind maximum with a northerly component is selected as the absolute maximum in the entire smoothed profile.
4. The SALLJ maximum wind speed and its height are defined as the observed (not smoothed) maximum wind speed present 500 m around the height of the wind maximum selected in step 3.

Figure 3 shows a noisy wind profile at Santa Cruz de la Sierra with the selection criteria applied. From this case, the wind profile is classified as SALLJ with a wind speed maximum of 15.2 m s^{-1} at 1700 m AMSL (1330 m AGL).

In agreement with Montini et al. (2019), the SALLJ wind speed maximum is highly dependent on the station where it is observed (Fig. 4). For example, half of the observed maxima wind speeds at Mariscal Estigarribia (80 profiles), Roboré (12 profiles), and Santa Cruz de la Sierra (51 profiles) stations were stronger than 15 m s^{-1}, but only 15% exceeded that value at Rio Branco (5 profiles), Chamical (10 profiles), and Cruzeiro do Sul stations (2 profiles). The greater northerly wind speed observed around Mariscal Estigarribia can be attributed to the SALLJ core located in this region (Salio et al., 2002; Marengo et al., 2004; Algarra et al., 2019; Montini et al., 2019), an aspect that will be discussed in the following Section. The evolution of the LLJ in terms of wind speed maximum, vertical wind shear, and intermittent turbulence have a complex interdependence in the nocturnal boundary layer. Besides, Montini et al. (2019)

found that the Bonner wind shear threshold higher than 6 m s^{-1} is too high for the SALLJ. Therefore, adhering to a fixed criterion for wind shear may unnecessarily limit the number of SALLJ cases. Bonner (1968) selected the LLJ cases with different thresholds for the maximum wind with the lowest value of 12 m s^{-1}. This value is close to the 50th percentile in most SALLJEX stations (Fig. 4). Montini et al. (2019) selected the LLJ cases using the 75th percentiles of wind speed at each station without discriminating between intensities. In the present work, the SALLJs were locally classified as weak when the SALLJ maximum wind speed was between the 55th and 70th percentile, moderate when the SALLJ maximum wind speed was between the 70th and 85th percentile, and strong when the SALLJ was higher than the 85th percentile. Using this criteria, correct SALLJ wind profiles were chosen without including profiles with a very weak wind maximum lower than their median (50%).

The analysis of the evolution of the LLJ was done for daytime (15, 18, and 21 UTC) and nighttime (03, 06, and 09 UTC) hours. Transition hours were classified based on the static stability at the level of the jet maximum thus, 00 UTC (12 UTC) was classified as after sunset (sunrise), this aspect is described in Section 4.1.1. It should be noted that there is a zone time difference of 1 hour between the SALLJEX stations, for most regions LT is UTC - 3h except LT at Bolivia and west-central Brazil is UTC - 4h. However, given the observational time resolution of the SALLJEX network, this time difference does not have an impact on the classification of transition hours.

Boundary layer heights were visually determined from the mean thermodynamic profiles. The boundary layer structure can be classified into three major regimes depending on the atmospheric thermodynamic environment (Stull, 1988): convective boundary layer (CBL), nocturnal stable boundary layer (NBL), and residual layer (RL). In this work, the CBL is determined as the layer from the near-surface up to the base of the entrainment zone where a pronounced decrease

in moisture and an increase in wind speed are observed. As diurnal convective turbulence dominates within this layer, constant virtual potential temperature and mixing ratio profiles are expected. NBL is determined as the layer from the near-surface to the height where the thermal inversion layer ends. At night under clear sky conditions, the surface cooling due to radiative deficit causes a statically stable layer with weaker and sporadic turbulence. Lastly, RL is determined as the nearly neutral layer from the NBL´s top to the height where similar conditions as for the CBL´s top are observed. This layer is characterized by uniformly mixed properties remaining from the previous CBL after the decoupling caused by the NBL stability.

4. Mean variables during the SALLJEX period

4.1. Wind temporal variation

Mean wind and thermodynamic profiles for each station for the SALLJEX period are analyzed. Given the greater number of observations homogeneously distributed during the day at Vilhena, Santa Cruz de la Sierra, Córdoba, and Resistencia (Fig. 2), the time-height variation of the mean wind speed and direction are analyzed in these stations to represent the north, west, south, and east regions respectively (Fig. 5). The mean wind speed maximum below 3000 m AMSL occurs mostly during night hours), between 03 UTC and 12 UTC at Vilhena, Córdoba, and Resistencia, in agreement with the inertial oscillation (Blackadar, 1957). Consistent with Marengo et al. (2002), Santa Cruz de la Sierra shows a persistent strong wind speed every hour except at 21 UTC. The different result found by Douglas et al. (1998) is explained mainly by the larger number of morning soundings (09-12 UTC) launched during the SALLJEX in comparison to the reduced quantity used in their study at 11-13 UTC. The weak wind speeds present at 09 UTC between 800 m and 2200 m AMSL are likely not representative of the mean wind behavior in this region but a consequence of having only 2

observations available (Fig. 2). Wind direction near the height of maximum wind speed remains steady from the north-northwest at Santa Cruz de la Sierra, while an anticlockwise wind rotation with a northerly domain is clearly seen at Córdoba (at 1100 m AGL between 00 and 09 UTC) Vilhena (at 900 m AGL between 03 and 15 UTC) and Resistencia (at 450 m AMSL between 03 and 15 UTC). The hodographs of the mean daily wind speed anomaly are calculated as the mean difference between the hourly wind speed and the respective daily mean for each component. The hodographs at Vilhena, Córdona, and Resistencia display an anticlockwise rotation with time at the maximum wind level (Figs. 5e, 5g- h). This behavior is similar to the semi-circular hodograph with respect to the geostrophic wind and its anticlockwise rotation from sunset to sunrise in a pure inertial oscillation (Blackadar, 1957). Resistencia hodograph has an elliptical shape with its major axis in the north-south direction (Fig. 5h). This hodograph shape is likely the result of the LLJ associated with geostrophic wind in the presence of a meridionally-oriented mountain range (e.g., Bonner and Paegle, 1970; Shapiro and Fedorovich, 2009). This behavior is less evident at the other sites in Figure 5 but it is apparent at other stations over the plains east of the Andes (not shown). Irregular hodograph patterns like the one depicted at Córdoba (Fig. 5g) or the northwest-southeast orientation of the hodograph at Santa Cruz de la Sierra (Fig. 5f) can be explained by blocking effects at sites near the Andes or by the thermally forced local circulations (Repinaldo et al., 2015). In the last case, depending on the magnitude of the mountain-plain breeze with respect to the zonal component derived from the inertial oscillation, these components can have opposite effects at 06 and 18 UTC and complementary effects at12 and 00 UTC. These results are similar to the ones found for the Great Plains low-level jet where a smoother clockwise rotation of the wind was found within the jet core and in contrast more chaotic hodographs at its border related to topographical effects (Zhong et al., 1996).

Data from Santiago del Estero (Fig. 6) is analyzed in more detail herein because of its proximity to the Andes (Fig. 1), its greater number of SALLJ profiles (Fig. 4), and because the observations are evenly distributed during the day (Fig. 2). Weaker winds during the daytime hours (15, 18, and 21 UTC) are likely a result of the CBL turbulent mixing leading to a more uniform magnitude in the wind profiles. The mean wind speed maximum is observed at 09 UTC at 700 m AMSL (~500 m AGL) and it is mostly due to an increase in the northerly wind (Figs. 6a-c). The wind speed diurnal oscillation between 500 and 2000 m AMSL results from the oscillation of both wind components (Fig. 6). The hodograph of the mean daily wind anomaly describes an elliptical shape with its major axis in the north-south direction (Fig. 6d). This hodograph shares characteristics with both Resistencia and Santa Cruz de la Sierra (Figs. 5f-h) according to Santiago del Estero's location between the plains east of the Andes and the Andes slopes.

4.2. Geographical variation of LLJ´s intensity and height

To describe the horizontal structure of the SALLJ by exploring a possible dependence of the LLJ wind speed maximum to latitude and distance from the Andes mountain range, mean wind speed vertical profiles are analyzed in different transects following the mountain barrier (Fig 7). 12 and 21 UTC are chosen as representative hours of the behavior of the wind speed at a time near its maximum and minimum respectively due to having the highest number of wind profiles in most of the stations at these times. The wind speed at 12 UTC is stronger than at 21 UTC for most stations (except Chamical, Figs. 7a-c) which is in agreement with Blackadar (1957). The daytime wind maximum observed at Chamical can probably be related to complex local terrain which can mask the inertial oscillation. Similar behavior was found by Inzunza and Berri (1991) at Salta, who suggested a dominance of mountain breezes over the inertial oscillation in the

diurnal wind cycle on the slopes of the Andes as a possible explanation. The low-level wind speed maximum at Santa Cruz de la Sierra, also seen at Rio Branco, is still present in hours when convective mixing is expected; however, this maximum is not as intense as the one at 12 UTC, in agreement with Marengo et al. (2002). Paegle (1998) suggested a latent heating contribution to buoyancy oscillations related to a nocturnal maximum in convective cloudiness near the Andes as a possible explanation for the late afternoon wind maximum at Santa Cruz in the observations documented by Douglas et al. (1998). There is evidence of weaker maxima at 21 UTC at the same height of maxima at 12 UTC in the profiles along the eastern transect (Fig 7c). Similar behavior was found by Inzunza and Berri (1991) at Resistencia and it might be explained as a weakening of the 12 UTC maximum or as an initiation of the nocturnal oscillation cycle at higher latitudes where the inertial oscillation period is shorter. The strongest mean wind speed is observed at Roboré in the central transect (Fig 7b), reaching a mean wind peak speed of 15 m s^{-1} at 12 UTC. At this station, most of the measurements were done during IOPs, on days when an intense SALLJ event was expected. Therefore, mean SALLJEX profiles at this station are likely biased by strong cases.

In the western transect, an intensification of the wind is observed from Rio Branco to Santa Cruz de la Sierra followed by a weakening poleward towards Chamical (Fig. 7a). Wind speed over the central and east transects shows a similar behavior but with a stronger poleward weakening from Roboré to Tostado (Fig. 7b) and from Dourados to Resistencia (Fig. 7c). The LLJ weakening with latitude is dependent on the location of the SALLJ core (Nicolini et al, 2005; 2006). Also, it can be related to the increase in transient activity with the penetration of summer frontal systems affecting more frequently the stations located in the southern sector of the SALLJEX region.

At stations at a similar latitude, the mean wind speed maxima decrease eastward, from the highest values at the stations closer to the Andes (Fig. 7a) to the lowest values at the eastern plains (Fig. 7c). This is likely associated with the effect of the Andes mountain range. Previous studies had shown the mechanical effect of the Andes for centering the SALLJ geographical core immediately eastward of the Andes and between Santa Cruz de la Sierra and Mariscal Estigarribia (Campetella and Vera, 2002; Byerle and Paegle, 2002). Proximity to a mountain range can also influence the LLJ via diabatic effects of differential heating/cooling over the sloping terrain (e.g., Holton, 1967; McNider and Pielke, 1981; Parish and Oolman, 2010; Parish, 2017; Shapiro et al., 2016).

Figure 7b-c shows a poleward decrease of the maximum wind speed height AGL along the LLJ (1350 m AGL at Mariscal Estigarribia, 540 m AGL at Pampa de los Guanacos, 525 m AGL at Tostado; 620 m AGL at Dourados, 610 m AGL at Asunción, 450 m AGL at Resistencia, 390 m AGL at Paraná). This can be because in stable nocturnal conditions the turbulence, and hence the height of the boundary layer, is largely generated by the wind shear associated with the LLJ (Van de Wiel et al., 2010). Thus, this poleward decrease of the LLJ height AGL could be due to the relationship between the LLJ core height and boundary layer height resulting in an inverse dependence on the height of the NBL and the Coriolis parameter (Li, 2013).

4.3. Spatial and temporal variation of the low-level thermodynamic profile

Differences in the thermodynamic vertical structure at stations located in tropical and subtropical regions may evidence the presence of different air masses. Figure 8 shows the mean temperature, virtual potential temperature, and specific humidity profiles at Santiago del Estero, Santa Cruz de la Sierra, Chamical, and Resistencia at 00, 06, 12, and 18 UTC. These stations are selected given their higher number of thermodynamic measurements distributed throughout the day

(Fig. 2a). These profiles are used as indicators of the static stability and to study its diurnal variation in this section. From these profiles, the CBL at Santa Cruz de la Sierra reaches the mean depth of 700 m at 18 UTC (Fig. 8f). Deeper CBLs are observed southward, over Chamical, Resistencia, and Santiago del Estero stations with 1500 m mean depths (Figs. 8e, and 8g-h). This difference at stations located near the orography or at a similar latitude over the plains to the east can be explained by large-scale mechanisms. For example, Nicolini et al. (2005, 2006) compared the thermodynamic vertical structure in LLJ events immersed in two different synoptic patterns named Chaco LLJ (CHJ) and LLJ Argentina (LLJA). They found that during CHJ events, a maximum LLJ at Santa Cruz de la Sierra and Mariscal Estigarribia was immersed in a low-level poleward flow that drove warm and humid advection toward subtropical northeastern Argentina (reaching Resistencia). On the other hand, LLJA revealed the presence of a northerly LLJ generated locally over subtropical northwestern Argentina (clearly depicted at Santiago del Estero) in the western sector of a postfrontal anticyclone located to the east of the Andes. According to these authors, it was during this second pattern that LLJs were the strongest at Santiago del Estero. Moisture and temperature advection in this postfrontal air mass was weaker during these events but clearer skies at Santiago del Estero and Chamical favored stronger radiational heating. This difference in air masses contributing to the mean thermodynamic structures is evident in the vertical specific humidity profiles at low levels near the Andes both at Santiago del Estero and Chamical (Fig 8a,c) with respect to Santa Cruz and Resistencia (Fig 8b,d) where a more humid boundary layer is shown during both day and night hours. Another factor that could modify the relationship between the height of the boundary layer and the latitude is the difference in the type of soil (Ruscica et al., 2020). Santiago del Estero and Chamical have mostly sandy/dryer soil while Resistencia has mainly clay/humid soil with vegetation.

This aspect may affect the diurnal surface energy balance and therefore the thermodynamic profile and height of the convective boundary layer.

At 06 UTC, the NBL at Santiago del Estero reaches 600 m AGL, above which the virtual potential temperature profile is less stable. The temperature profile shows a shallow thermal inversion below 300 m AGL. A notable difference in the virtual potential temperature profiles would be expected between the NBL and the RL above but this behavior is not observed in Santiago del Estero. The layer between 600 and 2000 m AGL corresponding to the RL shows a stable vertical profile at 06 UTC (Fig. 6e). This can be due to the effect caused by the average of profiles with different daytime CBL and NBL depths. Another possible explanation is that strong wind shear around the maximum wind speed can cause mechanical turbulent fluxes that can lead to strong vertical mixing in regions of high wind speed (Van de Wiel et al, 2010; Klein et al 2015). This vertical mixing prevails between the NBL and the RL, thus permitting vertical transport while coupling the layers (e.g., Acevedo et al., 2012; Hu et al., 2013).

The thermodynamic profiles at 12 UTC (00 UTC) show stability conditions much more similar to the profiles at 06 UTC (18 UTC) (Fig. 8), thus this transition hour is considered stable (unstable) in the following analyses. The mixing ratio profile composites show a diurnal cycle with a minimum at daytime near the surface but without evident nocturnal changes between 06 and 12 UTC (Fig. 8). This diurnal minimum can be the result of vertical turbulent mixing during the hours of insolation in the absence of horizontal advection or processes that involve phase changes of water. This mixing is more efficient near the surface as a constant specific humidity is not attained in the convective layer. There are many possible reasons for the lack of a constant specific humidity profile in the CBL. One of them is associated with cloudy days that would not have a mixed boundary layer as compared to profiles from clear days and plenty of incoming solar radiation. Another possible reason for the lack of a constant profile and the lack

of evident nocturnal changes is related to the effect that average could cause in different daily profiles with a large variability of the boundary layers top leading to heterogeneous vertical profiles.

5. Characterization of the SALLJ by categories

5.1. Frequencies of occurrence

With the aim of exploring the main characteristics of the SALLJ depending on its intensity, the SALLJ strength is categorized at each SALLJEX site using percentile thresholds of wind speed maximum. Figure 9 shows the relative frequency of occurrence of all SALLJ categories. In order to analyze robust statistics, stations having at least 4 hours with more than 9 observations are analyzed. This condition represents 10% of the possible total observations if all observations were collected every day at each hour. Relative frequencies are calculated with the quantity of SALLJ profiles on each category divided by the number of total wind profiles performed per hour at each station (Fig. 2b). Frequencies at hours and stations with less than 10 observations are not included in the following analysis. Vilhena, Rio Branco, and Dourados do not have many measurements but they are uniformly distributed throughout the day. At most other stations there are more observations between 09 and 21 UTC, particularly at 12 and 21 UTC (Fig. 2). Overall, the timing of SALLJs is likely dependent on their intensity; weak SALLJ frequencies are quasi-homogeneous or larger at early (15 UTC, Vilhena) or late (21 UTC, Pampa de los Guanacos) afternoon (Fig. 9). In the moderate category, frequencies are higher during the early morning hours (06 to 12 UTC, Tostado and Asunción) with a secondary maximum near sunset (21 UTC at Córdoba and 00 UTC at Resistencia). Strong SALLJs are more frequent at 06-12 UTC at all stations, with the highest frequency at 06 UTC at Paraná and Resistencia; 09 UTC at Joaquín V. Gonzalez, Mcal. Estigarribia, Pampa de los Guanacos, Dourados, Tostado and Vilhena; and 12 UTC at

Asunción and Santa Cruz de la Sierra. The only exception is Chamical, as discussed in Section 4.1., this behavior is possibly related to the mean maximum wind speed found during daytime hours. Therefore, weak SALLJs that occur at any time of the day can be related to different low-level phenomena and occur independently of a nocturnal inertial oscillation. In some cases, they can be the residual wind maxima of a previous strong nocturnal SALLJ affected by convective turbulence. Particularly at Pampa de los Guanacos, 10 of the 12 daytime weak SALLJ profiles were preceded by nocturnal strong and moderate cases (figure not shown). On the other hand, strong SALLJs frequently occur at nighttime hours, likely in connection with the decoupling of the RL (Blackadar, 1957).

5.2. Diurnal variability of the SALLJ wind profiles

With the aim of exploring the differences in wind speed maximum height between SALLJ categories as well as its diurnal cycle, SALLJ wind speed profiles for different categories and times at Santiago del Estero station are shown in Figure 10. For all categories, fewer SALLJ cases occur during the maximum insolation hours (15, 18, 21 UTC), as discussed in the previous subsection. Figure 10 shows no substantial differences in the maximum height of nocturnal cases between categories. The maximum height of nocturnal SALLJs can mostly be found between 500 and 1000 m AMSL (300 and 800 m AGL) and they can reach heights as high as 2000 m AMSL (1800 m AGL). On the other hand, the height of the daytime SALLJs reaches 1500 and 3000 m AMSL (1300 and 2800 m AGL). Little can be said about differences in the maximum height of daily cases between categories due to low number of cases. Weak and moderate SALLJs reach their mean maximum height at 2000 m AMSL (1800 m AGL) at 18 UTC. Particularly, for weak SALLJ, a lower secondary maximum appears at 21 UTC and at 1200 m AMSL (1000 m AGL) at 21 UTC.

The height of the maximum wind speed increases after sunrise for all SALLJ categories at Santiago del Estero. This result can be seen in the moderate category and was also observed in Mariscal Estigarribia, Pampa de los Guanacos, Tostado and Asunción (not shown). Most of these profiles correspond to the same days (mostly since the first IOP), so this diurnal behavior can be favored by the vertical transport of horizontal momentum. Krishna (1968) and Jiang et al. (2007) noted that the vertical phase tilt of the LLJ is dependent on latitudes. They found that upper levels in the boundary layer are ahead of lower levels in reaching the peak in the wind speed at latitudes higher than 30º. After sunset, friction is reduced at relatively high levels and the inertial oscillation can begin earlier and consequently, the maximum wind speed can also be reached earlier. But, the longer inertial period in the stations at lower latitudes leads to an interruption of this oscillation due to the activation of the turbulent mixture at sunrise starting near the surface. In this way, the upper boundary layer levels above had more time to reach the maximum, which lead to the diurnal phase of the maximum wind having a tendency to tilt positively in time-height cross-sections as in Figure 10 from Jiang et al. (2007). This behavior is consistent with the one observed in the latitude band corresponding to the SALLJEX network mostly located north of 30ºS.

5.3. Differences in the boundary layer thermodynamic structure

A relationship between the SALLJ intensity and its thermodynamic properties of the lower layers of the atmosphere is presented in this section. Figure 11 shows the mean virtual potential temperature, temperature, and specific humidity profiles for the 3 categories at 06 UTC from nights with SALLJ and at 18 UTC from the previous day at Santiago del Estero and Resistencia. These stations are selected due to a larger number of thermodynamic profiles at 06 and 18 UTC, a larger quantity of nocturnal SALLJ cases, and in order to represent the

different synoptic patterns and the related thermodynamic structure at these locations discussed in Section 4.3. Virtual potential temperature and temperature composites at both stations at 06 UTC vary between categories (Fig 11a-d). Stronger heating in the layer up to 700 hPa in strong and moderate cases compared to weak cases is noticeable. This is probably a result of warm advection carried by the SALLJ from lower latitudes. Particularly in the strong cases at Resistencia (Figs. 11b and 11d), this advection above the maximum wind speed height seems to contribute to a deeper and stronger inversion layer (strong stability) at lower levels, similar to the profiles previously referred to as CHJ in section 4.3. CHJ events have stronger wind and higher temperature at Resistencia because they are immersed in a poleward flow that drives warm and humid air toward subtropical northeastern Argentina (Nicolini et al. 2002; Salio et al, 2002). This mechanism can oppose and dominate the turbulent fluxes generated by wind shear around the strong winds that lead to a less stable NBL. In fact, heating above wind speed maximum cannot be seen and a less stable NBL is noted in weak cases. Differences can be found in Santiago del Estero composites (Figs. 11a and 11c), which depict weaker warm transport than at Resistencia, coherent with profiles categorized as LLJA. LLJA events were generated in the western sector of a postfrontal anticyclone located to the east of the Andes, thus moisture and heat transport in this postfrontal air mass were weaker during these events while clear skies favor stronger radiational heating (Nicolini et al, 2005; 2006).

Composite profiles at 18 UTC from the previous day where nocturnal SALLJ was observed at 06 UTC show a higher mean temperature and a deeper CBL in the strong cases than the weak cases (Figs. 11a-b). Consistent with Blackadar's theory (1957), stronger heating during insolation hours leads to a deeper and more turbulent CBL that generates a larger difference between the geostrophic wind and the total wind at the decoupling time. These results suggest that the nocturnal inertial oscillation is one of the local mechanisms that generates

and controls the SALLJ. Figure 11e depicts drier lower levels at 18 UTC at Santiago del Estero in moderate and strong cases than in the weak ones (Fig. 11a). At Resistencia for the strong SALLJs, the humidity profile at 18 UTC is mixed, possibly caused by efficient convective turbulence which leads to drying at the surface and moistening at upper levels (Fig. 11f). During night hours, the horizontal moisture advection at lower levels may generate a moistening at 06 UTC that is not present during weak and moderate SALLJs.

6. Summary and Conclusions

An observational analysis of the SALLJ during the SALLJEX at 21 stations located along the SALLJ axis was performed. This study analyzes some aspects of the horizontal structure of the SALLJ that had not been already explored by previous studies and aspects of the diurnal wind cycle, height, and timing of the maximum wind over this broad region east of the Andes that previous authors only had pointed out for a few isolated locations. Progress in the characterization of the SALLJ will improve understanding of moisture fluxes and moisture budget over SESA that are still not adequately represented by gridded data. With that motivation, a relationship between the SALLJ strength and the low-level vertical thermodynamic structure was explored in this work. Kinematic and thermodynamical analyses of different SALLJ intensities require a new definition of SALLJ from wind profiles that have a local maximum with a northerly component below 3000 m AMSL. Wind speed maxima depict a strong variability between stations, revealing the need for not fixed thresholds in SALLJ identification criteria as Montini et al. (2019) argued in their study. Weak, moderate, and strong categories were determined using the 55, 70 and 85 percentiles from the wind speed maxima distribution at each station.

Mean SALLJEX time-height diagrams were used to characterize wind features related to the diurnal cycle, height and timing of wind maxima, and its

spatial variation over the network. Observations at Vilhena, Santa Cruz de la Sierra, Córdoba, and Resistencia stations show stronger wind speeds in the lower levels of the troposphere (below 3000 m AMSL) at night hours or near dawn (from 03 UTC to 12 UTC). Due to the lack of information during night hours and the discretized measurements every 3, 6 or 12 hours, the precise hour of wind speed maximum can not be determined. At stations with more observations at nighttime, the maximum wind speed is found between 06 and 12 UTC and it is mainly from the north. This agrees with results found by Inzunza and Berri (1991) at Resistencia despite different time periods being analyzed. The mean wind time-height diagram at Santa Cruz de la Sierra shows stronger winds both night and day with a weakening at 21 UTC. This result agrees with Marengo et al. (2002) but not with Douglas et al. (1998). Possible reasons for this are the reduced number of morning soundings used by the latter authors and the use of a different study period. In the present study, the only exception to the nocturnal maximum wind speed is observed at Chamical, which shows stronger winds at 21 UTC. Hodographs of mean daily wind anomaly describe an anticlockwise rotation with time at the height of the maximum wind speed. The wind speed maximum timing and the anticlockwise rotation can be an indicator that the inertial oscillation has an important role in the wind's diurnal cycle over the SALLJ. Stronger wind speeds are mainly from a northerly direction, thus hinting that the SALLJ had a strong signature in the average of the entire SALLJEX period.

The geographical variation of LLJ´s intensity and height over a broad region east of the Andes is studied purely from observations in this work for the first time. The maximum mean wind speed present at Santa Cruz de la Sierra and Roboré, suggests the presence of the LLJ core near this latitudinal band (~ 19°S). This result agrees with previous observational (Marengo et al. 2002) and model (Salio et al. 2002; Saulo et al. 2002) studies. From the analysis presented in this work, a weakening of the maximum wind speed is observed from stations near

the Andes to stations eastward over the plains. This suggests a possible mechanical effect of the Andes on centering the SALLJ geographical core, in agreement with previous studies (Campetella and Vera, 2002; Byerle and Paegle, 2002; Silvers and Schubert, 2012). The analysis shows a poleward decrease of the maximum wind speed height AGL along the jet stream. Despite some differences in the maximum wind height and depth found at different stations, the height of the maximum wind speed could be found mostly from 300 m AGL to 2000 m AGL. The highest altitude of the maximum wind speed (around 2000 m) found in some stations suggests the presence of elevated LLJs. This result is in agreement with previous studies (Saulo et al, 2004; 2007; Oliveira et al. 2018, Sasaki et al. 2022).

The higher frequencies of SALLJ profiles vary between categories and stations. Weak SALLJs are mostly homogeneously distributed throughout the day, while moderate SALLJs present higher frequencies between 06 and 12 UTC with the maximum at 09 UTC at particular stations. Resistencia has a secondary maximum near sunset time that is associated with the weaker daytime maximum already found in previous studies (Inzunza and Berri, 1991). On the other hand, strong SALLJs occur during night hours between 06 and 12 UTC at all stations, except at Chamical. Therefore, the strongest SALLJs are frequently found during night hours, in agreement with the inertial oscillation theory (Blackadar, 1957). The thermodynamic characterization of the boundary layer shows several differences between SALLJ categories at Santiago del Estero and Resistencia. A deeper CBL and a greater mean temperature at strong and moderate cases rather than weak cases are found at both stations during the previous afternoon (18 UTC) to nocturnal SALLJs (06 UTC). Consequently, intense SALLJs seem to be favored by an inertial oscillation of higher amplitude at the decoupling time caused by stronger heating during insolation hours. Near the time of wind speed maximum (06 UTC), a more stable NBL is found in moderate and strong cases as

compared to weak cases. Warm advection associated with the SALLJ itself in strong cases can also contribute to the warmer observed profile with a deeper inversion layer compared with the moderate SALLJ cases. The results that arise from this analysis are consistent with profiles described in previous studies (Nicolini et al, 2002; 2005; 2006; Salio et al, 2002) under different synoptic patterns.

Many open questions remain after the comprehensive SALLJ analysis presented in this work for a particular warm season. These results should not be considered as a 'climatology' of the LLJ east of the Andes. Additional observational resources, such as wind profilers, are needed to improve the wind characterization, overcoming temporal sampling limitations inherent to a pibal and radiosonde network. Important relationships were found between SALLJ and atmospheric stability and inferred turbulence in the boundary layer, topography, and large-scale flow patterns. To complete the analysis and improve future results, it is convenient to study variables that represent turbulence, temperature advection, and diabatic effects related to cloudiness, among other processes. Evaluation of different reanalyses of low-level circulations and other related products like nocturnal precipitation and wind maxima is still needed in all the SALLJEX network. Also, temporal and spatial resolution coherence is extremely important to correctly study the diurnal wind cycle in this region with such complex topography.

Acknowledgments

The authors acknowledge the scientists, students, collaborators, and local volunteers that participated in the planning, execution, and data analysis effort for SALLJEX.

SALLJEX was funded by NOAA/OGP, NSF (ATM0106776), and funding agencies from Brazil (FAPESP Grant 01/13816-1), collaborative program IAI-

CRN 55 and from Argentina (ANPCyT PICT 07-1757 and 07-06671, UBA X30 and X055). It was also supported by PACS-SONET network. Further SALLJEX datasets quality controls have been partially funded by Argentina Projects ANPCyT PICT 07-14420, CONICET PIP 5582 and UBA X266.

Additional support was provided by the U.S. Department of Energy Office of Science Biological and Environmental Research as part of the Atmospheric System Research program. Pacific Northwest National Laboratory is operated by Battelle for the U.S. Department of Energy under Contract DE-AC05-76RLO1830.

The authors also thank two anonymous reviewers and Associate Editor Jose Marengo for their helpful comments and suggestions that improved the manuscript.

References

Acevedo, O.C., Costa, F.D., Degrazia, G.A., 2012. The coupling state of an idealized stable boundary layer. Boundary-Layer Meteorology 145(1):211–228. doi:10.1007/s10546-011-9676-3

Algarra, I., Eiras-Barca, J., Nieto, R., Gimeno, L., 2019. Global climatology of nocturnal low-level jets and associated moisture sources and sinks. Atmos. Res. 229, 39–59. doi: 10.1016/j.atmosres.2019.06.016

Arkell, R.E., 2000. Differentiating between types of wind shear in aviation forecasting. National Weather Digest, 24:3, 39-51.

Arraut, J. M., Nobre, C., Barbosa, H. M. J., Obregon, G., Marengo, J., 2012. Aerial rivers and lakes: Looking at large-scale moisture transport and its relation to Amazonia and to subtropical rainfall in South America. Journal of Climate, 25, 543–556. https://doi.org/10.1175/2011JCLI4189.1.

Arya, S. P., 2005. Micrometeorology and Atmospheric Boundary Layer. Pure and Applied Geophysics, 162 (10), 1721–1745. doi:10.1007/s00024-005-2690-y

Blackadar, A. K., 1957. Boundary-layer wind maxima and their significance for the growth of nocturnal inversions. Bulletin of the American Meteorological Society, 38 (5), 283-290. https://doi.org/10.1175/1520-0477-38.5.283

Bonner, W. D., 1968. Climatology of the Low Level Jet. Monthly Weather Review. 96 (12), 833-850. https://doi.org/10.1175/1520-0493(1968)096<0833:COTLLJ>2.0.CO;2

Bonner, W. D., Paegle, J., 1970. Diurnal Variations in Boundary Layer Winds Over the South Central United States in Summer. Monthly Weather Review, 98, 735-744. doi:10.1175/1520-0493(1970)098<0735:DVIBLW>2.3.CO;2

Braz, D. F., Ambrizzi, T., da Rocha, R. P., Algarra, I., Nieto, R., & Gimeno, L., 2021. Assessing the moisture transports associated with nocturnal low-level jets in continental South America. Frontiers in Environmental Science, 9, 657764, https://doi.org/10.3389/fenvs.2021.657764

Byerle, L. A., J. Paegle, 2002. Description of the seasonal cycle of low-level flows flanking the Andes and their interannual variability. Meteorologica, 27, 71–88, 2002.

Campetella, C., Vera, C., 2002. The influence of the Andes Mountains on the South American low level flow. Geophysical Research Letters. 29 (17), 1826. doi:10.1029/2002GL015451

Douglas, M, Nicolini, M., Saulo, C., 1998. Observational evidences of a low level jet east of the Andes during January-March 1998. Meteorologica, 23, 63-72.

Fernandez, A. and G. Necco, 1982. Wind characteristics in the free atmosphere at Argentinian radiosounding stations (in Spanish) . Meteorologica 13(2); 7-21.

Gálvez, J.M., Orozco, R., Douglas, M., 2005. Measuring and monitoring the mesoclimate of tropical locations. Field observations from the South American Altiplano during the salljex. Project Pacs Sonet.

García Skabar, Y., and M. Nicolini, 2009: Enriched Analyses with Assimilation of SALLJEX Data. J. Appl. Meteor. Climatol., 48, 2425–2440. doi:10.1175/2009JAMC2091.1

Gimeno, L., Dominguez, F., Nieto, R., Trigo, R., Drumond, A., Reason, C.J.C., Taschetto, A.S., Ramos, A.M., Kumar, R., Marengo, J., 2016. Major Mechanisms of Atmospheric Moisture Transport and Their Role in Extreme Precipitation Events. Annual Review of Environment and Resources, 41(1). doi:10.1146/annurev-environ-110615-085558

Gutierrez, W., Araya, G., Basu, S., Ruiz-Columbie, A., Castillo, L., 2014. Toward Understanding Low Level Jet Climatology over West Texas and its Impact on Wind Energy. Journal of Physics: Conference Series. 524, 012008. doi:10.1088/1742-6596/524/1/012008

He, Y., Sheng, Z., Zhou, L., He, M., Zhou, S., 2020. Statistical analysis of turbulence characteristics over the tropical western pacific based on radiosonde data. Atmosphere (Basel). 11, 1–20. https://doi.org/10.3390/ATMOS11040386

Holton, J. R., 1967. The diurnal boundary layer wind oscillation above sloping terrain. Tellus, 19, 199-205. https://doi.org/10.1111/j.2153-3490.1967.tb01473.x

Hu X-M., Klein, P.M., Xue, M., Lundquist, J.K., Zhang, F., Qi, Y., 2013. Impact of low-level jets on the nocturnal urban heat island intensity in Oklahoma City.

Journal of Applied Meteorology and Climatology. 52 (8), 1779–1802. https://doi.org/10.1175/JAMC-D-12-0256.1

Inzunza, B. J., Berri, G. J., 1991. Wind behavior and water vapor transport in the lower troposphere in northern Argentina (in Spanish). Meteorologica. 17, 17 – 25.

Jiang, X., Lau, N.-C., Held, I. M., Ploshay, J. J., 2007. Mechanisms of the Great Plains low level jet as simulated in an AGCM. Journal of Atmospheric Sciences. 64, 532–547. doi:10.1175/JAS3847.1

Jones, C., 2019. Recent changes in the South America low-level jet. NPJ Clim. Atmos. Sci. 2, 1–8. doi: 10.1038/s41612-019-0077-5

Klein, P. M., Hu, X.M., Shapiro, A., Xue, M. 2015: Linkages between boundary Layer structure and the development of nocturnal Low Level Jets in central Oklahoma. Boundary-Layer Meteorology. 158, 383–408. https://doi.org/10.1007/s10546-015-0097-6

Krishna, K., 1968. A numerical study of the diurnal variation of meteorological parameters in the planetary boundary layer. Monthly Weather Review. 96 (5), 269-276. https://doi.org/10.1175/1520-0493(1968)096<0269:ANSOTD>2.0.CO;2

Li, W., 2013. Stable boundary layer height parameterization. Learning from artificial neural networks. Atmospheric and Climate Sciences. 3 (4), 523-531. doi: 10.4236/acs.2013.34055.

Lichtenstein, E. R., 1980. La Depresion del Noroeste Argentino (The Northwestern Argentina Low). Ph.D. dissertation, University of Buenos Aires, 223 pp.

Madougou, S., Saïd, F., Campistron, B., Kebe, C.F., 2014. Low Level Jet Wind Shear in the Sahel. International Journal of Engineering Research in Africa, Trans Tech Publications, 2014, 11, pp.1-10. ff10.4028/www.scientific.net/JERA.11.1ff. ffhal-00979942f

Marengo, J. A., Douglas, M. W., Dias, P. L. S., 2002. The South American low-level jet east of the Andes during the 1999 LBA-TRMM and LBA-WET AMC campaign. Journal of Geophysical Research Atmospheres. 107(D20), 8079. doi:10.1029/2001JD001188

Marengo, J. A., Soares, W. R., Saulo, C., Nicolini, M., 2004. Climatology of the low-level jet east of the Andes as derived from the NCEP-NCAR reanalyses: Characteristics and temporal variability. Journal of Climate.17(12), 2261-2280. https://doi.org/10.1175/1520-0442(2004)017<2261:COTLJE>2.0.CO;2

McNider, R. T., Pielke, R. A., 1981. Diurnal boundary-layer development over sloping terrain. Journal of Atmospheric Sciences, 38(10), 2198-2212. https://doi.org/10.1175/1520-0469(1981)038<2198:DBLDOS>2.0.CO;2

Means, L. L., 1954. A study of the mean southerly wind—Maximum in low levels associated with a period of summer precipitation in the Middle West. Bull. Amer. Meteor. Soc.,35, 166–170.

Montini, T. L., Jones, C., Carvalho, L. M. V., 2019. The South America Low-level Jet: new climatology, variability and changes. Journal of Geophysical Research: Atmospheres. 124, 1200-1218. https://doi.org/10.1029/2018JD029634

Nascimento, M.G., Herdies, D.L., Souza, D.O., 2016. The South American water balance: The influence of low-level jets. Journal of Climate. 29(4), 1429-1449. https://doi.org/10.1175/JCLI-D-15-0065.1

Nicolini, M., Saulo, A. C., 2000. Eta characterization of the 1997-1998 warm season Chaco jet cases. Sixth Int. Conf. On Southern Hemisphere Meteorology and Oceanography, Santiago, Chile. American Meteorological Society. 330-331.

Nicolini, M., Saulo, A.C., Torres, J. C. , and P. Salio, 2002. Strong South America low-level jet events characterization during warm season and implications for enhanced precipitation. Meteorologica, 27, 59–69.

Nicolini, M., Salio, P., Borque, P., 2005. Characterization of the thermal and kinematic vertical structure of the lower troposphere in northern Argentina during SALLJEX (in Spanish). Ninth Congreso Argentino de Meteorología, Buenos Aires, Argentina, Centro Argentino de Meteorólogos, CD-ROM.

Nicolini, M., Salio, P., Borque, P., 2006: Thermodynamic and Kinematic Characterization of the Low Level Troposphere During the SALLJEX Under Different Large Scale Environments. Eighth International Conference on Southern Hemisphere Meteorology and Oceanography, Foz do Iguaçu, Brazil, Abril 24-28, 2006, p.1141-1148.

Oliveira, M. I., Nascimento, E. I., Kannenberg, C., 2018. A New Look at the Identification of Low Level Jets in South America. Monthly Weather Review. 146(7), 2315-2334. https://doi.org/10.1175/MWR-D-17-0237.1

Parish, T. R., Oolman, L.D., 2010. Notes and Correspondence on the Role of the Sloping Terrain in the Forcing of the Great Plains Low Level Jet. Journal of the Atmospheric Sciences. 67(8), 2690-2699. doi: 10.1175/2010JAS3368.1

Parish, T. R., 2017. On the Forcing of the summertime Great Plains low-level Jet. Journal of the Atmospheric Sciences. 74(12), 3937-3953. https://doi.org/10.1175/JAS-D-17-0059.1

Rife, D. L., J. O. Pinto, A. J. Monaghan, C. A. Davis, and J. R. Hannan, 2010. Global distribution and characteristics of diurnally varying low-level jets. J. Climate., 23, 5041–5064, https://doi.org/10.1175/2010JCLI3514.1

Rasmussen, K. L., Houze, R.A. Jr., 2011. Orogenic convection in subtropical South America as seen by the TRMM satellite. Monthly Weather Review. 139, 2399-2420. https://doi.org/10.1175/MWR-D-10-05006.1

Rasmussen, K. L., Zuluaga, M. D., Houze, R. A., Jr., 2014. Severe convection and lightning in subtropical South America. Geophysical Research Letters. 41, 7359-7366. doi:10.1002/2014GL061767.

Rasmussen, K. L., Houze, R. A., Jr., 2016. Convective initiation near the Andes in subtropical South America. Monthly Weather Review. 144(6), 2351-2374. https://doi.org/10.1175/MWR-D-15-0058.1

Repinaldo, H. F. B., Nicolini, M., García Skabar, Y., 2015. Characterizing the diurnal cycle of low-level circulation and convergence using CFSR data in southeastern South America. Journal of Applied Meteorology and Climatology. 54, 671-690. doi:10.1175/JAMC-D-14-0114.1

Repinaldo, H. F. B., Nicolini, M., García Skabar, Y., 2017. Convective storm initiation over the sierras de Córdoba and sensitivity to changes in the orographic profile (in Spanish). Meteorologica. Vol. 42, Nº2, 23-42.

Ruscica, R.C., Polcher, J., Salvia, M.M., Sörensson, A.A., Piles, M., Jobbágy, E.G. Karszenbaum, H., 2020. Spatio-temporal soil drying in southeastern South America: the importance of effective sampling frequency and observational errors on drydown time scale estimates. International Journal of Remote Sensing. 41(20), 7958-7992. doi: 10.1080/01431161.2020.1767825

Ryan, W.B.F., Carbotte, S.M., Coplan, J.O., O'Hara, S., Melkonian, A., Arko, R., Weissel, R.A., Ferrini, V., Goodwillie, A., Nitsche, F., Bonczkowski, J., Zemsky, R., 2009. Global Multi-Resolution Topography synthesis. Geochemestry, Geophysics, Geosystems. 10, Q03014. doi: 10.1029/2008GC002332

Salio, P., Nicolini, M., Saulo, A.C., 2002. Chaco low-level jet events characterization during the austral summer season. Journal of Geophysical Research. 107(D24), 4816. doi:10.1029/2001JD001315.

Salio, P., Nicolini, M., Zipser, E. J., 2007. Mesoscale convective systems over southeastern South America and their relationship with South American low-level jet. Monthly Weather Review, 135(4), 1290-1309. https://doi.org/10.1175/MWR3305.1

Saulo, C., Nicolini, M., Chou, S. C., 2000. Model characterization of the South American low-level flow during the 1997–1998 spring–summer season. Climate Dynamics. 16, 867–881. doi:10.1007/s003820000085.

Shapiro, A., Fedorovich, E., 2009. Nocturnal low-level jet over a shallow slope. Acta Geophysica. 57, 950-980. https://doi.org/10.2478/s11600-009-0026-5

Shapiro, A., Fedorovich, E., Rahimi, S., 2016. A unified theory for the Great Plains nocturnal low level jet. Journal of the Atmospheric Sciences. 73(8), 3037-3057. https://doi.org/10.1175/JAS-D-15-0307.1

Silvers, L. G., and W. H. Schubert, 2012. A theory of topographically bound balanced motions and application to atmospheric low-level jets. J. Atmos. Sci., 69, 2878–2891, https://doi.org/10.1175/JAS-D-11-0309.1.

Stull, R.B., 1988. Mean Boundary Layer Characteristics. In: Stull, R.B. (eds) An Introduction to Boundary Layer Meteorology. Atmospheric Sciences Library, vol 13. Springer, Dordrecht. https://doi.org/10.1007/978-94-009-3027-8_1

Stensrud, D.J., 1996. Importance of low-level jets to climate: A review, Journal of Climate. 9(8), 1698- 1711. https://doi.org/10.1175/1520-0442(1996)009<1698:IOLLJT>2.0.CO;2

Sugahara, S., da Rocha, R.P., Rodrigues, M. L., 1994. Atmospheric conditions associated with the South America low level jet (in Portuguese). Seventh Congresso Brasileiro de Meteorologia, Vol. 2, Belo Horizonte, Brazil, Brazilian Meteorological Society, 573–577.

Ulke, A. G., Longo, K. M., Freitas, S. R., 2011. Biomass burning in South America: transport patterns and impacts, in Biomass-Detection, Production and Usage, D. Matovic, InTech, Rijeka, Croatia, 2011. doi: 10.5772/19264

Van de Wiel, B. J. H., Moene, A. F., Steeneveld, G. J., Baas, P., Bosveld, F. C., Holtslag, A. A. M., 2010. A conceptual view on inertial oscillations and nocturnal low-level jets. Journal of the Atmospheric Sciences. 67(8), 2679–2689. https://doi.org/10.1175/2010JAS3289.1

Varble, A. C., Nesbitt, S. W., Salio, P., Hardin, J. C., Bharadwaj, N., Borque, P., DeMott, P. J., Feng, Z., Hill, T. C. J., Marquis, J. N., Matthews, A., Mei, F., Öktem, R., Castro, V., Goldberger, L., Hunzinger, A., Barry, K. R., Kreidenweis, S. M., McFarquhar, G. M., McMurdie, L. A., Pekour, M., Powers, H., Romps, D. M., Saulo, C., Schmid, B., Tomlinson, J. M., van den Heever, S. C., Zelenyuk, A., Zhang, Z., & Zipser, E. J. (2021). Utilizing a Storm-Generating Hotspot to Study Convective Cloud Transitions: The CACTI Experiment, Bulletin of the American Meteorological Society, 102(8), E1597-E1620.

Velasco, I., Fritsch, J.M., 1987. Mesoscale convective complexes in the Americas. Journal of Geophysical Research: Atmospheres. 92(D8), 9591 - 9613. doi:10.1029/JD092iD08p09591.

Virji, H., 1981. A preliminary study of summertime tropospheric circulation patterns over South America estimated from cloud winds. Mon. Weather Rev.: 109, 596-610.

von Engeln, A., Teixeira, J., 2013. A Planetary Boundary Layer Height Climatology Derived from ECMWF Reanalysis Data. Journal of Climate. 26(17), 6575-6590. https://doi.org/10.1175/JCLI-D-12-00385.1

Wei, W., Zhang, H., Wu, B., Huang, Y., Cai, X., Song, Y., Li, J., 2018. Intermittent turbulence contributes to vertical diffusion of PM2.5 in the North China Plain. Atmospheric Chemistry and Physics. 1–21. https://doi.org/10.5194/acp-18-12953-2018, 2018.

Zipser, E. J., Cecil, D. J., Liu, C., Nesbitt, S. W., Yorti, D. P., 2006. Where are the most intense thunderstorms on Earth? Bulletin of the American Meteorological Society. 87(8), 1057–1071. https://doi.org/10.1175/BAMS-87-8-1057

Zhong, S., J. D. Fast, and X. Bian, 1996. A case study of the Great Plains low-level jet using wind profiler network data and a high- resolution mesoscale model. Mon. Wea. Rev., 124, 785–806.

Table captions

Table 1: Timing for pibal and radiosonde data collected during SALLJEX

Figure captions

Figure 1: SALLJEX observational network. Stations where pibals (blue square), radiosondes (red circle), and pibals and radiosondes (green diamond) were launched, are shown. Markers with red lines represent radiosonde operative stations during the campaign. Information on the station elevation AMSL is provided in the legend. The SESA region is delimited by a dotted square. Topography (in meters) from Global Multi-Resolution Topography (Ryan et al., 2009) is also shown (shaded)

Figure 2: Number of (a) thermodynamic and (b) kinematic observations during the SALLJEX.

Figure 3: SALLJ profile selected by the criteria at Santa Cruz de la Sierra: observed wind profile (blue line), 5-point moving average wind profile (orange line), all the local maxima in the smoothed profile up to 3000 m (black circles) with their respective direction in degrees (black numbers), 500 m layer around the larger maximum with northerly direction (black dotted lines), SALLJ wind speed maximum and peak (black star).

Figure 4: Violin box plots of SALLJ wind speed maxima for each and all SALLJEX stations. The 55th, 70th, 85th percentiles, and mean value (black and red horizontal lines respectively) are shown for each violin box plot. Number of SALLJ profiles are shown on the top (red numbers).

Figure 5: (a-d) Time-height diagrams of SALLJEX mean wind speed (shaded) and horizontal wind direction (vectors) and (e-h) hodographs of the daily mean wind anomaly (rings are delimited each 1 m s-1), at: (a, e) Vilhena, (b, f) Santa

Cruz de la Sierra, (c, g) Córdoba and (d, h) Resistencia. Mean hodographs of the daily wind anomaly are plotted at the heights denoted by the horizontal dotted lines drawn in the upper panels.

Figure 6: Mean vertical profiles at Santiago del Estero station. a) wind speed, b) zonal component of wind speed, c) meridional component of wind speed. Legends are shown at the bottom of each row with the number of averaged profiles in parenthesis. The hodograph of the daily average wind anomaly at 800 m AMSL is shown in the top right corner of the panel a) (rings are delimited each 1 m s^{-1}).

Figure 7: Mean wind speed profiles (m/s) grouped in transects at 12 UTC (full lines) and 21 UTC (dashed lines). a) Western transect, b) central transect (between a and c), c) eastern transect, calculated with the SALLJEX data for the entire measurement period. In the legends, the number of averaged profiles (12UTC, 21UTC) are in parentheses. In d) the locations of the stations included in each transect are shown with shapes and colors: a) (squares), b) (circles) and c) (crosses). Shaded topography (m) is shown.

Figure 8: Mean profiles of (a-d) temperature, (e-h) virtual potential temperature and (i-l) specific humidity at (a, e, i) Santiago del Estero, (b, f, j) Santa Cruz de la Sierra, (c, g, k) Chamical and (d, h, l) Resistencia for the SALLJEX period. In the legends, the number of averaged profiles is in parentheses for each hour and station. The shading delimits the standard deviation in the hours with more than 9 measurements.

Figure 9: Percentage of frequencies of occurrence of SALLJ relative to the number of measurements per hour for the weak, moderate and strong categories

at each station. Green numbers represent hours with more than 10% of existing data and red numbers represent the opposite case.

Figure 10: SALLJ profiles (colored lines) and their mean profile (black line) at each hour (columns) for each category (rows) at Santiago del Estero. Horizontal blue lines represent the mean SALLJ height and the numbers on the upper-right represent the quantity of SALLJ profiles plotted.

Figure 11: Composite profiles of (a, b) virtual potential temperature, (c, d) temperature and (e, f) specific humidity by categories at (a, c, e) at Santiago del Estero and (b, d, f) Resistencia at 06 UTC (solid lines) and previous 18 UTC (dotted lines) for the days with SALLJ at 06 UTC. The numbers in parentheses represent the quantity of profiles used to compute the composite (06 UTC; 18 UTC)

Table 1

Period	Dates	Pibal	Radiosonde
Regularly	Nov 15, 2002 to Feb 15, 2003	12, 21 UTC	06 UTC
SOP	Jan 6, 2003 to Feb 15, 2003	09, 12, 18, 21 UTC	06, 18 UTC
IOP	Jan 11, 12, 15-18, 21-25 and Feb 1, 2, 4-8, 11-15, 2003	00, 03, 06, 09,12, 15, 18, 21 UTC	00, 06, 12, 18 UTC

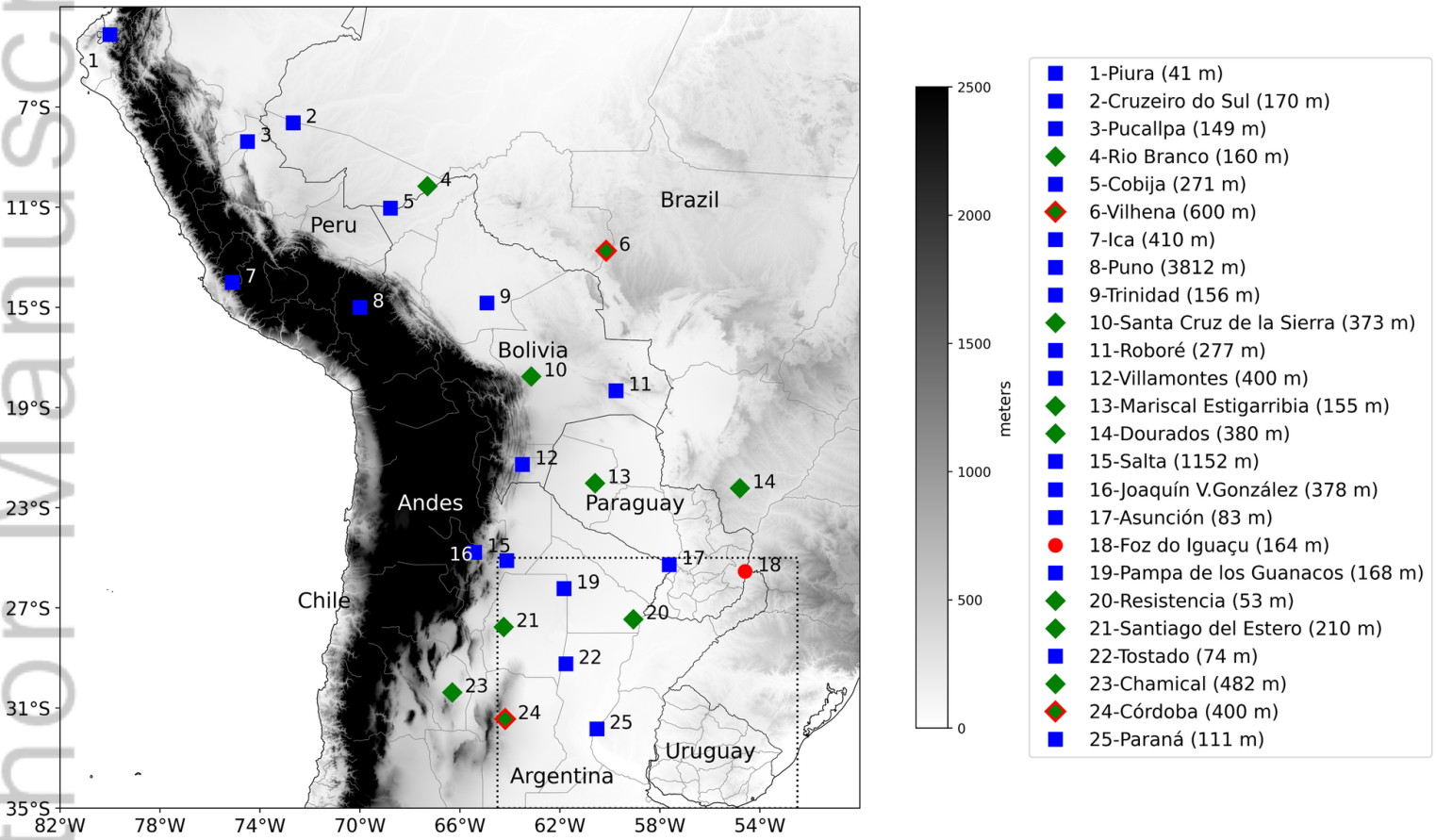

JOC_7857_fig_1_review.png

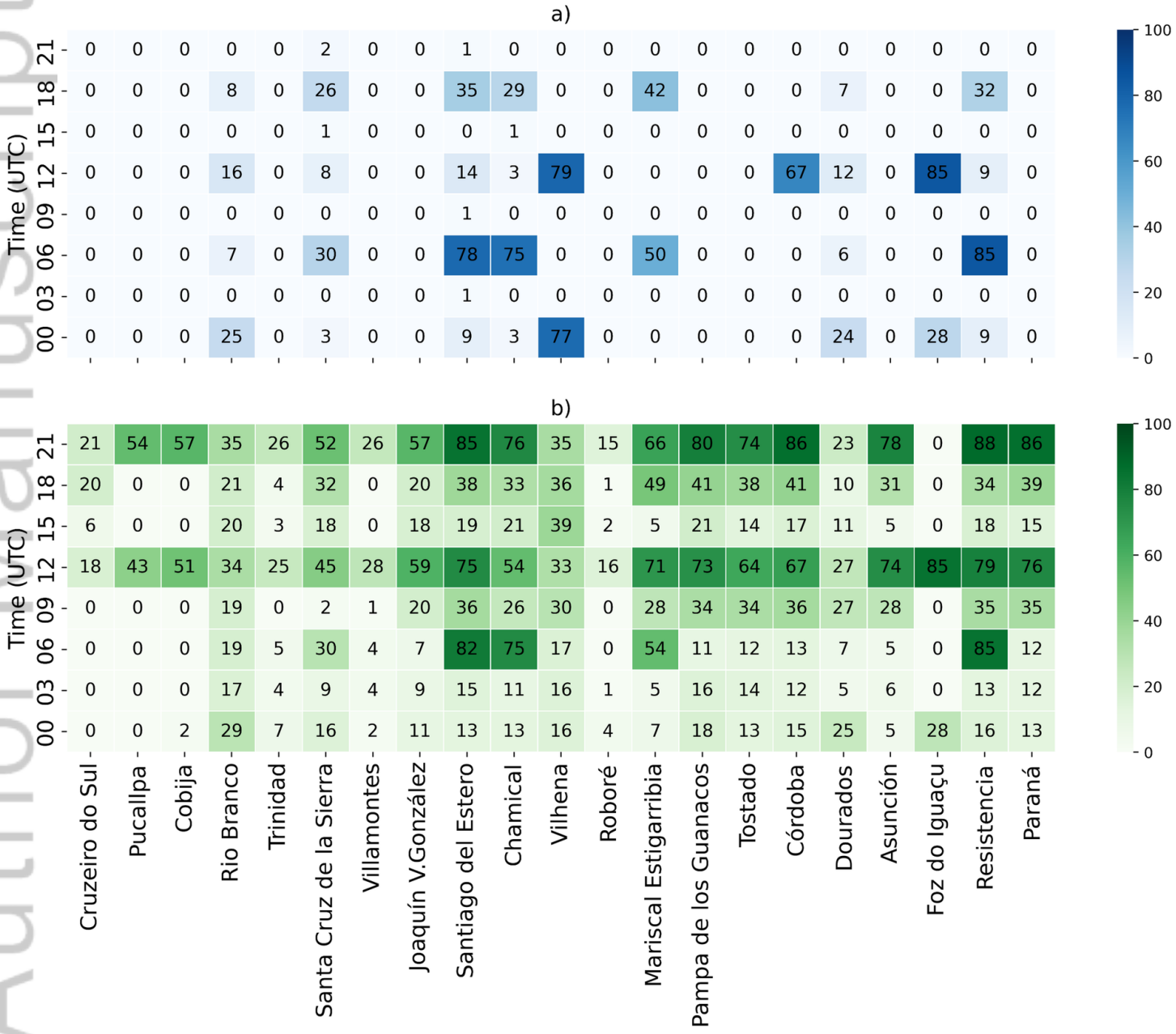

JOC_7857_fig_2_review.png

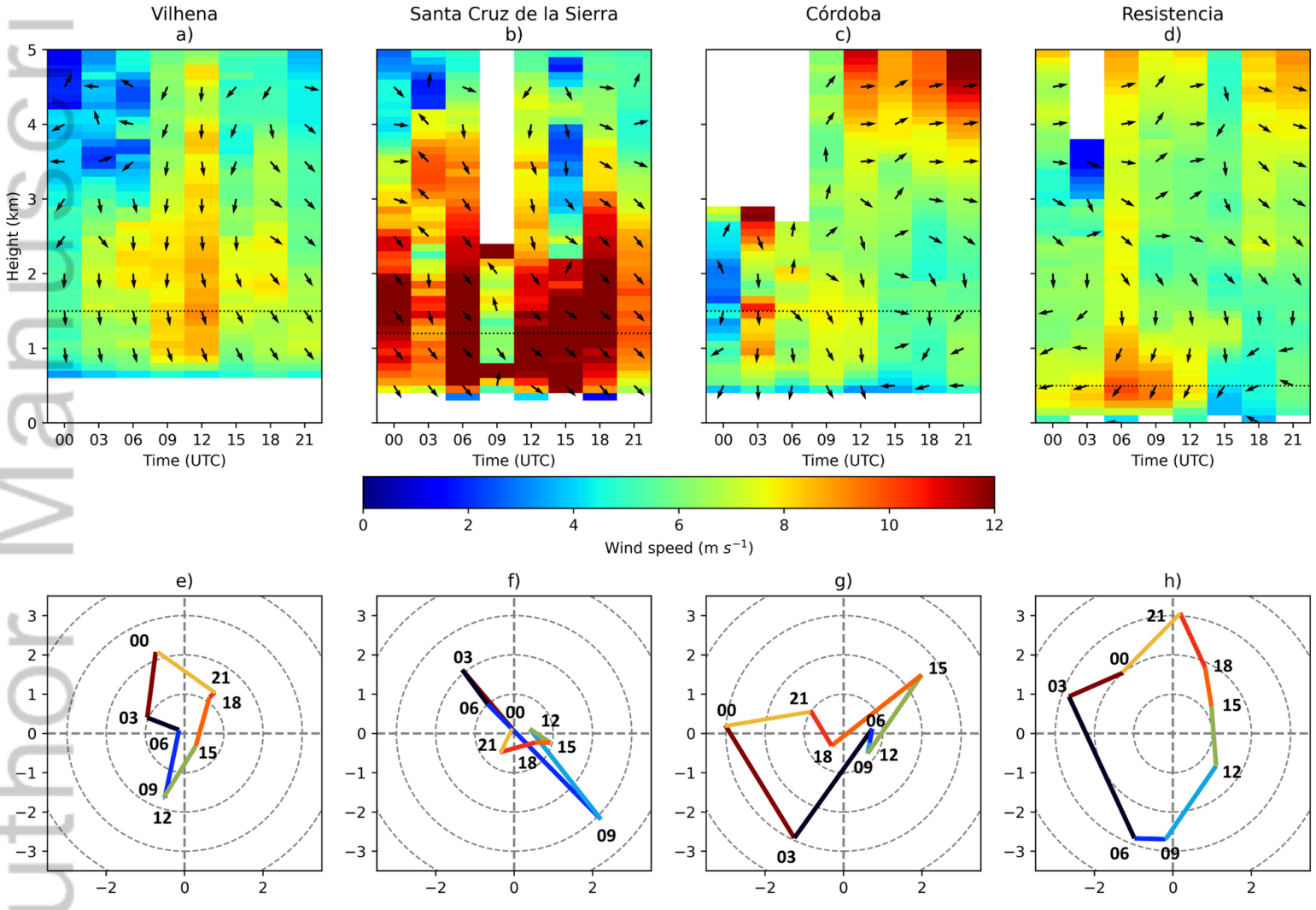

JOC_7857_fig_5_review.png

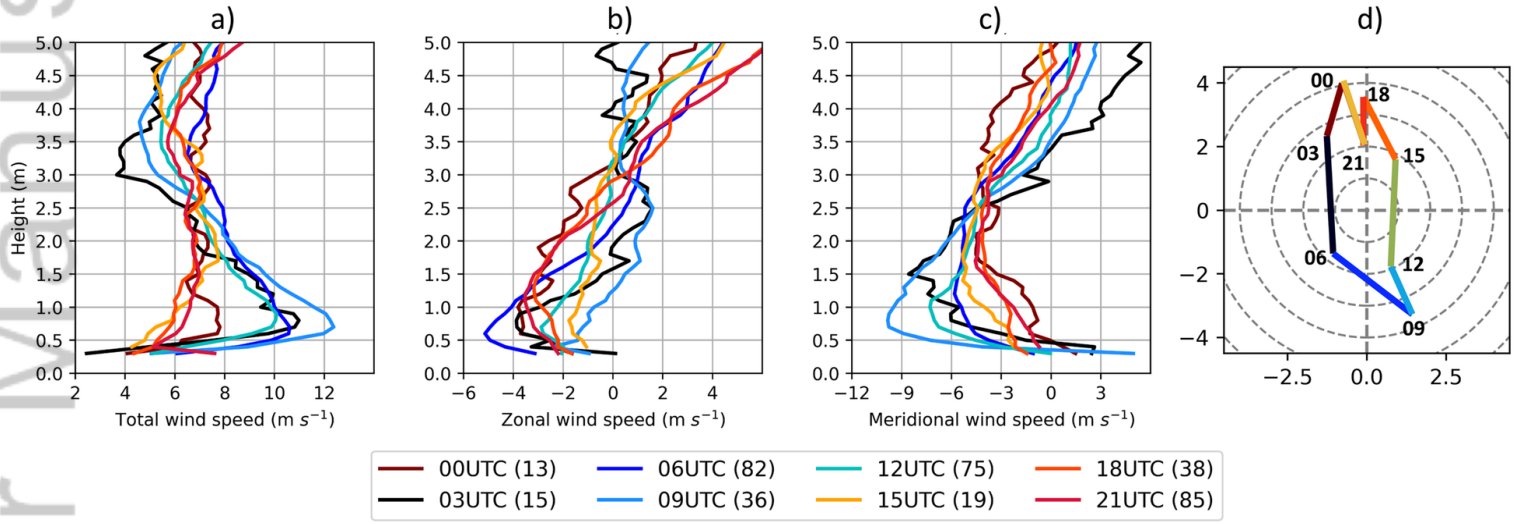

JOC_7857_fig_6_review.png

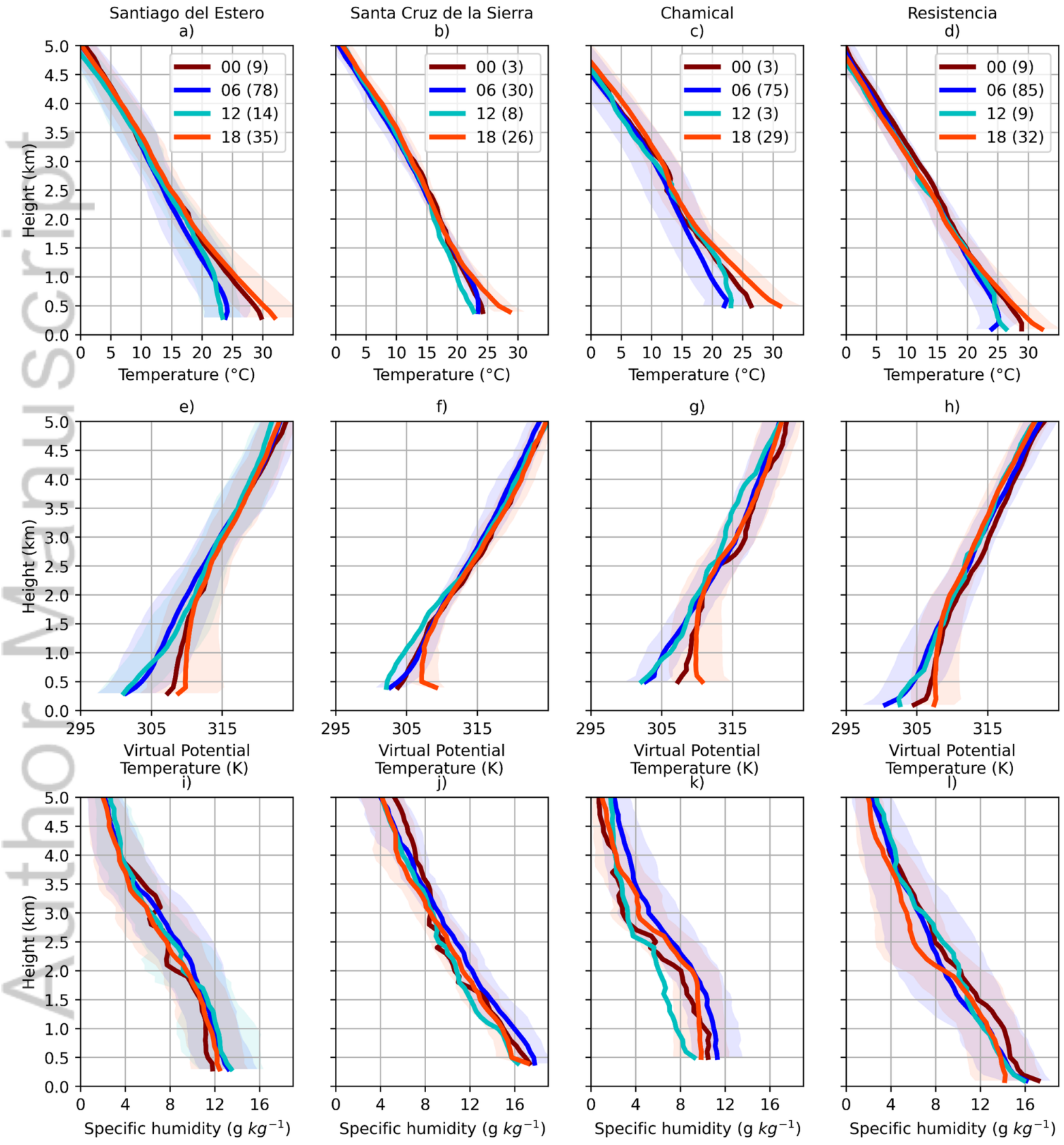

JOC_7857_fig_8_review.png

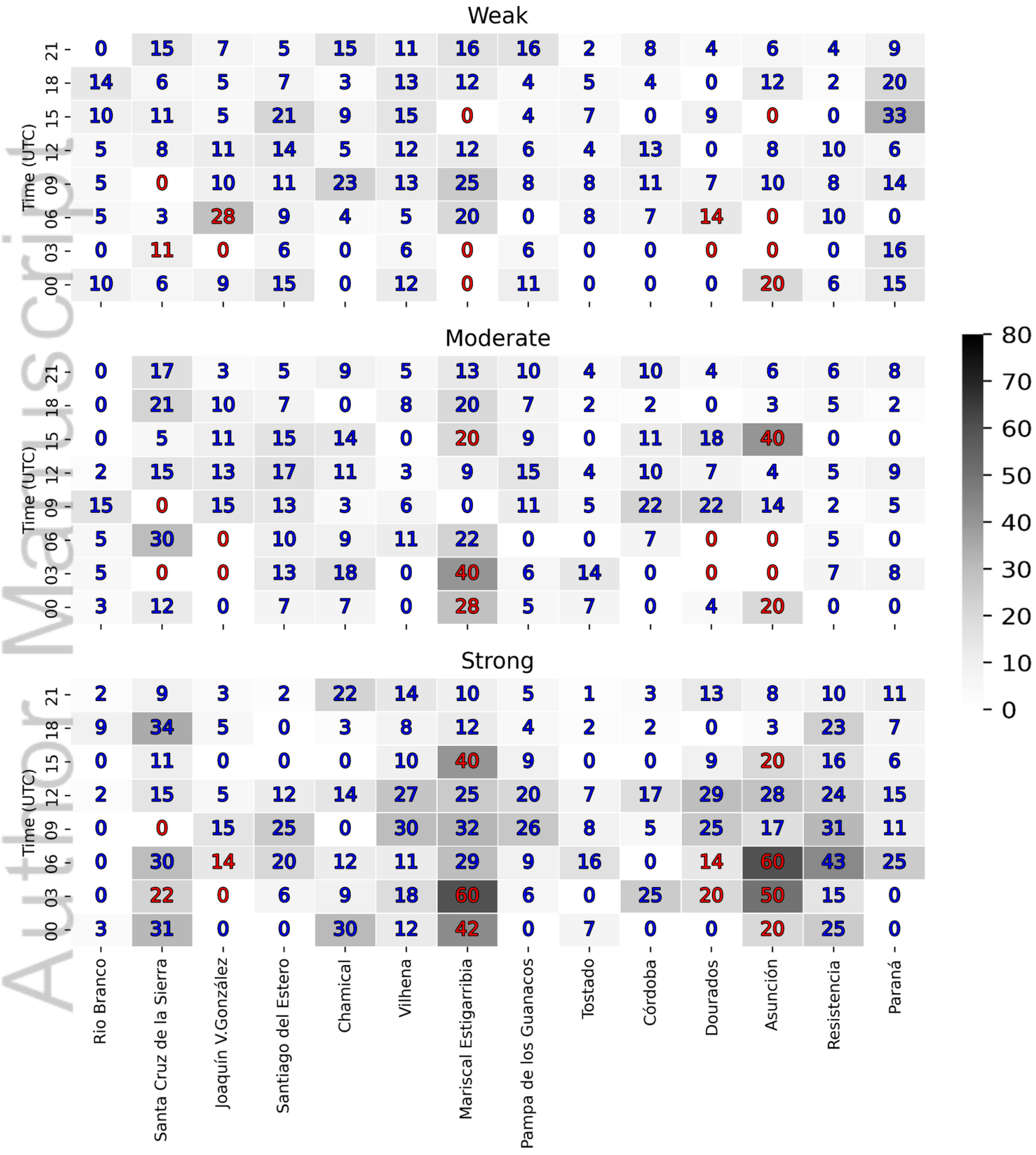

JOC_7857_fig_9_review.png

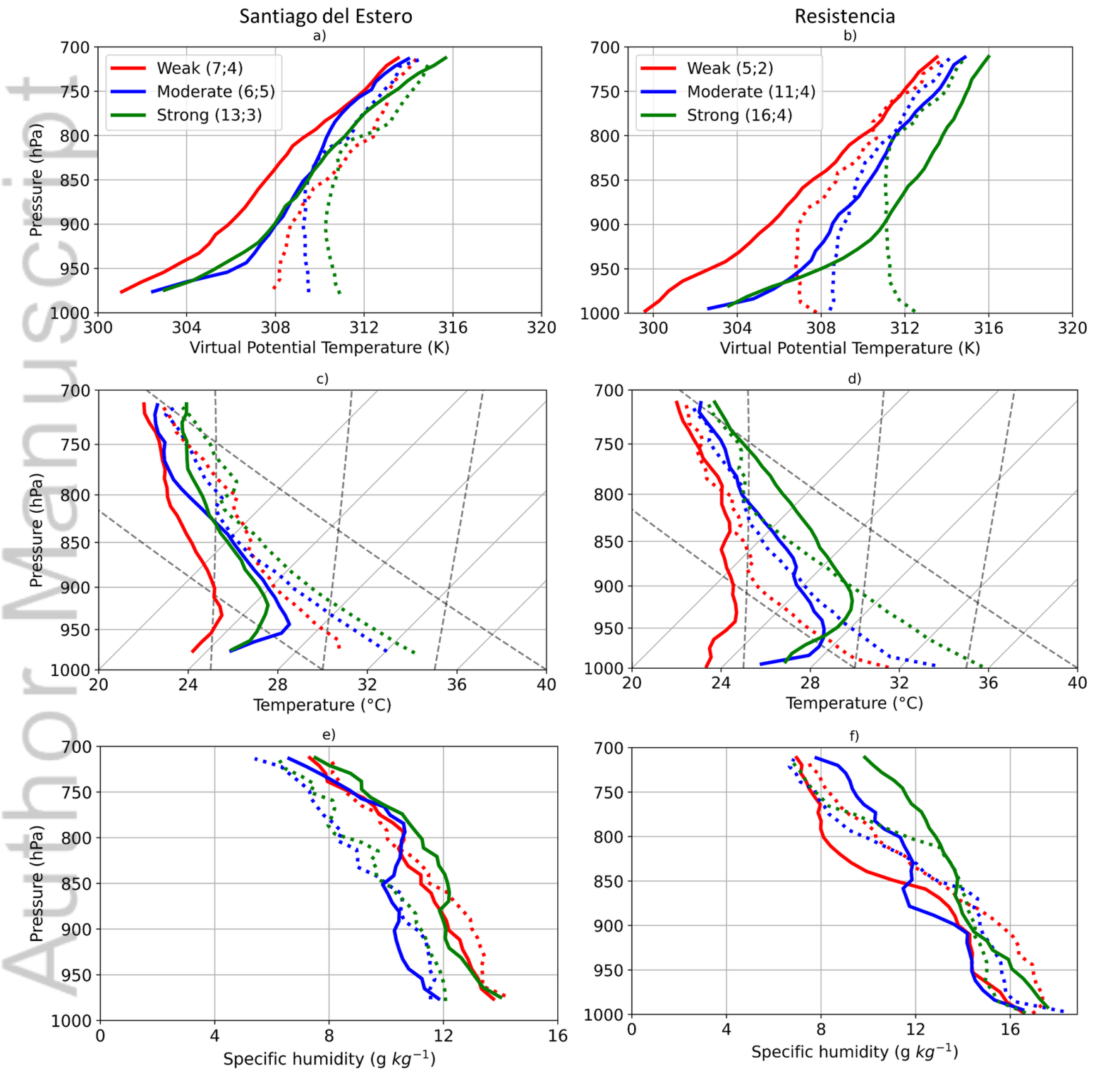

JOC_7857_fig_11_review.png

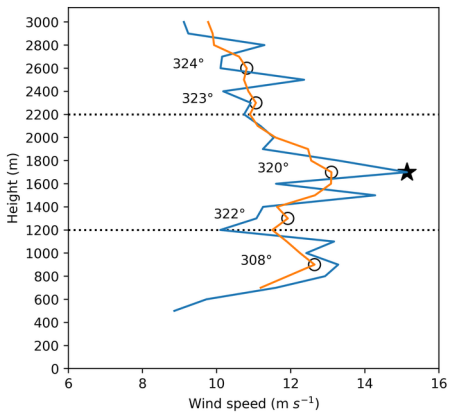

JOC_7857_fig__3.tif

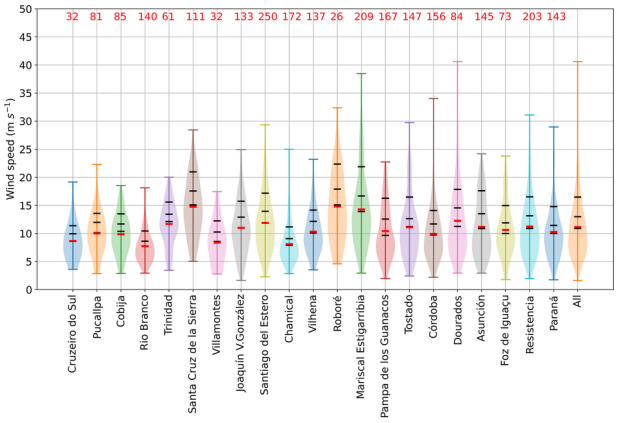

JOC_7857_fig__4.tif

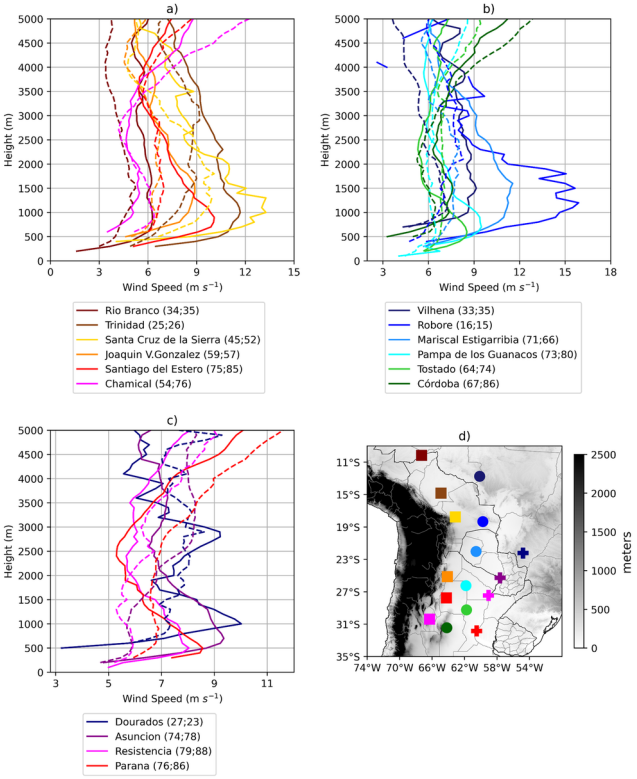

JOC_7857_fig__6.tif

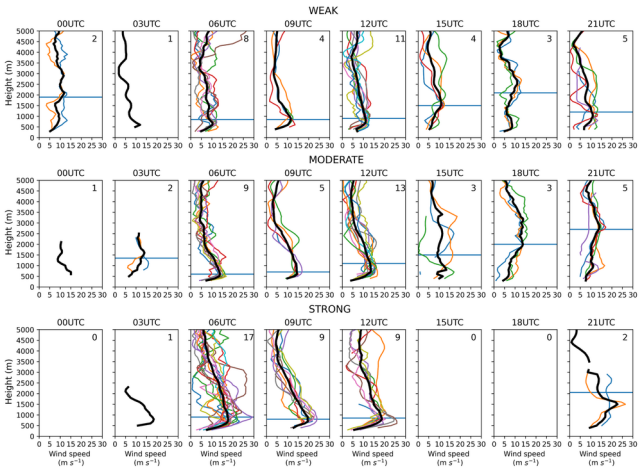

JOC_7857_fig__9.tif

Observational study of the South American Low-Level Jet during the SALLJEX

Yabra Melina Sol *, Matilde Nicolini, Paloma Borque, Yanina García Skabar, Paola Salio

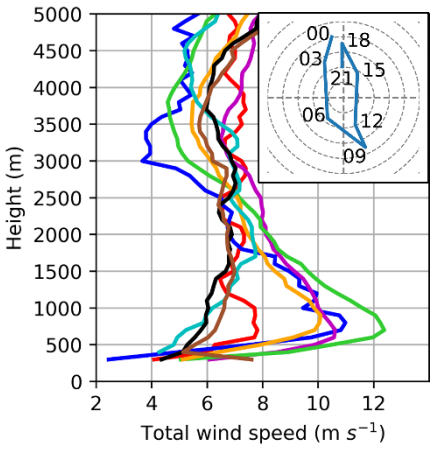

Higher wind speeds were observed below 3000 m between 06 and 12 UTC, and mostly in a northerly direction over SESA. The maximum wind speed was observed at around 17.8 °S and in proximity to the Andes Mountain range. Nocturnal SALLJs registered the greatest wind speeds whereas weaker SALLJs were found at any time of day. A deeper convective boundary layer and high mean temperature were observed at the afternoon previous to the occurrence of strong nocturnal SALLJs.

Table 1

Period	Dates	Pibal	Radiosonde
Regularly	Nov 15, 2002 to Feb 15, 2003	12, 21 UTC	06 UTC
SOP	Jan 6, 2003 to Feb 15, 2003	09, 12, 18, 21 UTC	06, 18 UTC
IOP	Jan 11, 12, 15-18, 21-25 and Feb 1, 2, 4-8, 11-15, 2003	00, 03, 06, 09,12, 15, 18, 21 UTC	00, 06, 12, 18 UTC